Colloquia: LC10

Higgs boson pair production in new physics models at hadron, lepton, and photon colliders(*)

K. Tsumura

National Taiwan University - Taipei, Taiwan

Summary. — We discuss Higgs boson pair production processes at future hadron and lepton colliders including the photon collision option in several new physics models, *i.e.* the two-Higgs-doublet model, the scalar leptoquark model, the sequential fourth-generation fermion model and the vectorlike quark model. Cross sections for these processes can differ significantly from the standard model predictions, due to the nondecoupling effect in the triple Higgs boson coupling constant. For the one-loop induced processes such as $gg \to hh$ and $\gamma\gamma \to hh$, new physics particles can mediate in a loop diagram, which can affect cross sections. Measurements of the Higgs boson pair production processes can be useful not only to test the standard model but also to explore new physics models.

PACS `12.60.Fr` – Extensions of electroweak Higgs sector.
PACS `14.80.Bn` – Standard-model Higgs bosons.

1. – Introduction

The standard model (SM) for particle physics is a successful model which can well describe phenomenology below electroweak scale. However, the last unknown particle, the Higgs boson, has not been discovered yet. Experimental search for the Higgs boson is the most important issues in the current high energy physics. The CERN Large Hadron Collider (LHC) has started its operation, and it is ready for hunting the Higgs boson. We expect that the Higgs boson will be discovered in the near future.

Once the Higgs boson is found, its property such as the mass, the decay width, production cross sections and the decay branching ratios will be thoroughly measured as accurately as possible. However, in order to understand the physics behind the electroweak symmetry breaking, experimental reconstructions of the Higgs potential is necessary by measuring the triple Higgs boson coupling constant (the *hhh* coupling constant).

(*) This proceeding paper is based on ref. [1].

From the theoretical view point, it is expected that the SM would be extended to a more fundamental theory at the TeV scale. One way to test the new physics effect is the precise measurement of effective vertices among the SM fields. The new physics contributions can affect to the effective vertices through radiative corrections. The effect can be substantial in the electroweak theory especially when the mass of a new particle comes mainly from the vacuum expectation value (VEV) of the Higgs field, *e.g.*, chiral fermions. In such a case the decoupling theorem [2] cannot be applied, so that the new physics effects are not necessarily decoupled and can be significant. It is well known that experimental bounds on the nondecoupling effects in radiative corrections to the gauge boson two-point functions are useful to constrain new physics models by using the precision data of electroweak parameters at the LEP and the Stanford Linear Collider (SLC) [3].

Such nondecoupling effects of new physics particles can also be very significant in the radiative corrections to the hhh coupling constant [4]. Quartic powerlike contributions of the mass of a new particle can appear in the one-loop correction to the hhh coupling constant, which can give a large deviation from the SM prediction. For example, in the two-Higgs-doublet model (THDM), the hhh coupling constant of the lightest (SM-like) Higgs boson can be deviated by $\mathcal{O}(100)\%$ due to nondecoupling effects of extra scalar bosons in radiative corrections without contradiction with perturbative unitarity [4]. The one-loop contributions to the hhh coupling constant can also be very large in the model with sequential fourth-generation fermions [5].

In this report, we summarize nondecoupling one-loop corrections to the hhh coupling constant in various new physics models such as the THDM, models with scalar leptoquarks, the model with the chiral fourth-generation fermions and the model with vectorlike quarks. We also discuss how the hhh coupling constant affects cross sections for the double Higgs boson production processes $gg \to hh$, $e^+e^- \to hhZ$, $e^+e^- \to hh\nu\bar{\nu}$ and $\gamma\gamma \to hh$.

2. – Nondecoupling effect on the Triple Higgs boson coupling constant

2·1. *Two-Higgs-doublet model.* – The potential of the THDM with a softly-broken discrete Z_2 symmetry is given by

$$(1) \quad V_{\text{THDM}} = m_1^2 \Phi_1^\dagger \Phi_1 + m_2^2 \Phi_2^\dagger \Phi_2 - \left(m_3^2 \Phi_1^\dagger \Phi_2 + \text{h.c.} \right) + \frac{\lambda_1}{2} \left(\Phi_1^\dagger \Phi_1 \right)^2 + \frac{\lambda_2}{2} \left(\Phi_2^\dagger \Phi_2 \right)^2$$
$$+ \lambda_3 \left(\Phi_1^\dagger \Phi_1 \right) \left(\Phi_2^\dagger \Phi_2 \right) + \lambda_4 \left(\Phi_1^\dagger \Phi_2 \right) \left(\Phi_2^\dagger \Phi_1 \right) + \left[\frac{\lambda_5}{2} \left(\Phi_1^\dagger \Phi_2 \right)^2 + \text{h.c.} \right],$$

where Φ_i $(i = 1, 2)$ are scalar isospin doublet fields with the hypercharge of $+1/2$, which transform as $\Phi_1 \to \Phi_1$ and $\Phi_2 \to -\Phi_2$ under the Z_2. Although m_3^2 and λ_5 are complex in general, we here take them to be real assuming the CP invariance. The two Higgs doublet fields can then be parameterized as

$$(2) \quad \Phi_i = \begin{pmatrix} \omega_i^+ \\ \frac{1}{\sqrt{2}}(v_i + h_i + i\, z_i) \end{pmatrix}.$$

The eight parameters m_1^2–m_3^2 and λ_1–λ_5 in the model are replaced by the VEV v, the mixing angle of CP even Higgs bosons α, the ratio of VEVs $\tan\beta = v_2/v_1$, the Higgs boson masses m_h, m_H, m_A, $m_{H^\pm}$ and the soft breaking parameter $M^2 = m_3^2/(\sin\beta\cos\beta)$.
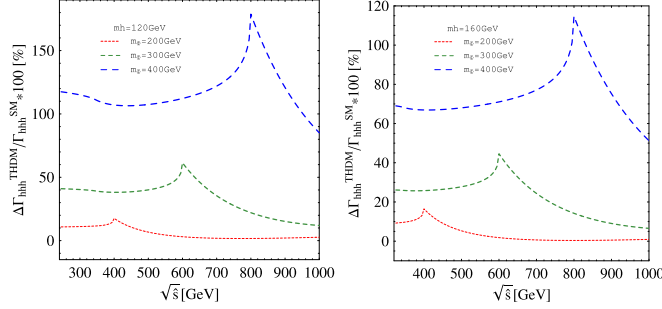
Fig. 1. – The rates for one-loop contributions from H, A, $H^\pm$ in the THDM to the hhh coupling constant for $m_h = 120\,\text{GeV}$ (left) and for $m_h = 160\,\text{GeV}$ (right).

Here, we consider the "SM-like" case with $\sin(\beta - \alpha) = 1$ where only the lighter CP-even Higgs boson h couples to the weak gauge boson as VVh [6]. In this case, all the coupling constants of h to the SM particles take the same form as those in the SM at the tree level. The hhh coupling constant is also described by the same tree-level formula as in the SM. The difference appears at the loop level due to the one-loop contribution of the extra scalars.

The one-loop correction to the hhh coupling constant in the THDM is evaluated as [4]

$$(3) \qquad \frac{\Gamma_{hhh}^{\text{THDM}}}{\Gamma_{hhh}^{\text{SM}}} \simeq 1 + \sum_{\phi = H, A, H^+, H^-} \frac{m_\phi^4}{12\pi^2 v^2 m_h^2} \left(1 - \frac{M^2}{m_\phi^2} \right)^3 .$$

The deviation from the SM results can be very large when $M^2 \simeq 0$. In fig. 1, the deviation in the effective hhh coupling constant from the SM value is shown as a function of $\sqrt{\hat{s}}$, the energy of $h^* \to hh$ in the THDM [4]. These effects can be significant, and the deviation in the hhh coupling constant can be approximately described by the analysis with a constant shift by the factor of $(1 + \Delta\kappa)$.

2`2. *Scalar leptoquarks*. – We next consider contributions to cross sections from scalar leptoquarks. Unlike the case with the extra Higgs scalar doublet, the scalar leptoquarks are colored fields. They, therefore, can affect the ggh and the $gghh$ vertices at the one-loop level. We here concentrate on a complex scalar, leptoquark, $\phi_{LQ} = (\bar{\mathbf{3}}, \mathbf{1})_{1/3}$ or $(\bar{\mathbf{3}}, \mathbf{1})_{4/3}$, as an example for such theories, where $SU(3)_C$, $SU(2)_L$ and $U(1)_Y$ quantum numbers are shown. The most general scalar potential can be written as

$$(4) \qquad V_{LQ}(\Phi, \phi_{LQ}) = \lambda \left(|\Phi|^2 - \frac{v^2}{2} \right)^2 + M_{LQ}^2 |\phi_{LQ}|^2 + \lambda_{LQ} |\phi_{LQ}|^4 + \lambda' |\phi_{LQ}|^2 |\Phi|^2,$$

where Φ is the SM Higgs doublet. The mass of leptoquarks is given by $m_{\phi_{LQ}}^2 = M_{LQ}^2 + \frac{\lambda' v^2}{2}$.

The one-loop correction to the hhh coupling constant due to the scalar leptoquark
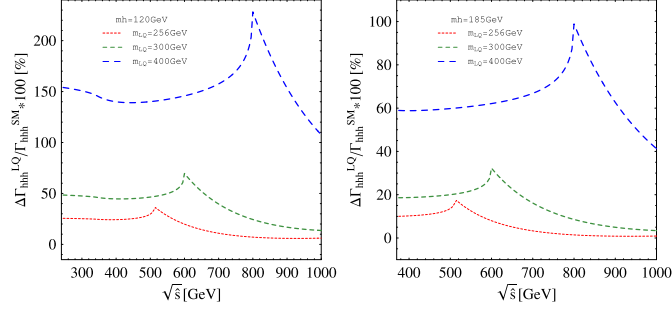
Fig. 2. – The rates for one-loop contributions of an $SU(2)$ singlet scalar leptoquark to the hhh coupling constant for $m_h = 120 \, \text{GeV}$ (left) and for $m_h = 185 \, \text{GeV}$ (right).

can be calculated analogous to the charged Higgs boson contribution in the THDM as

$$(5) \qquad \frac{\Gamma_{hhh}^{LQ}}{\Gamma_{hhh}^{SM}} \simeq 1 + \frac{N_c m_{\phi_{LQ}}^4}{6\pi^2 v^2 m_h^2} \left(1 - \frac{M_{LQ}^2}{m_{\phi_{LQ}}^2} \right)^3 .$$

In fig. 2, we evaluate the relative size of the one-loop contributions to the hhh coupling constant from the leptoquarks. These effects are constructive to the SM value in the nondecoupling region $M_{LQ}^2 \simeq 0$, which can be significant for heavy leptoquarks because of the $m_{\phi_{LQ}}^4$ enhancement.

2'3. Chiral fourth generation. – One of simplest extension of the SM is to introduce a sequential set of fermions. The large one-loop effect on the hhh coupling constant in the SM is generalized straightforwardly to the chiral fourth-generation model[1]:

$$(6) \qquad \frac{\Gamma_{hhh}^{Ch4}}{\Gamma_{hhh}^{SM}} \simeq 1 - \sum_{f'=t',b',\ell',\nu'} \frac{N_c m_{f'}^4}{3\pi^2 v^2 m_h^2} .$$

Since $m_{f'}^4$ enhancements come from extra heavy fermions, we would expect large quantum corrections to the hhh coupling constant. We note that these fermion loop contributions are always negative to the SM prediction. In fig. 3, effects of the chiral fourth generation fermions on the hhh coupling constant are shown. The hhh coupling constant is changed significantly depending on the energy of the off-shell Higgs boson.

2'4. Vectorlike quarks. – As a representative case of models for vectorlike quark, we adopt a pair of vectorlike up-type quarks, T_{0L} and T_{0R}, which transform as $(\mathbf{3}, \mathbf{1})_{2/3}$ under the gauge symmetry. The Lagrangian relevant to the mass of the SM top-quark and the vectorlike up-type quark can be written as

$$(7) \qquad \mathcal{L}^{\text{mass}} = -y_t \, \overline{Q}_0 \, t_{0R} \, \widetilde{\Phi} - Y_T \, \overline{Q}_0 \, T_{0R} \, \widetilde{\Phi} - M_T \, \overline{T}_{0L} T_{0R} + \text{h.c.},$$

where we have dropped the terms proportional to $\overline{T}_{0L} t_{0R}$ which are absorbed by redefinitions of t_{0R} and T_{0R} without loss of generality. Since the t_0–T_0 mixing term is allowed

---

[1] Neutrinos are assumed to be Dirac type whose masses are generated by Yukawa interaction.
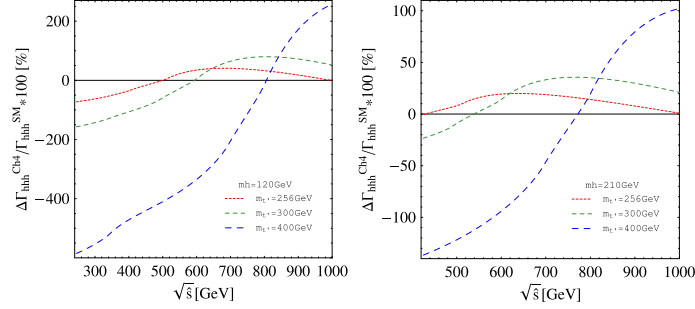
Fig. 3. – The rates for one-loop contributions of the chiral fourth generation fermions to the hhh coupling constant for $m_h = 120\,\text{GeV}$ (left) and for $m_h = 210\,\text{GeV}$ (right). The dotted, dashed, long-dashed curved lines indicate masses of heavy fermions as $m_{t'} = 256, 300, 400\,\text{GeV}$, respectively, with the appropriate mass difference $m_{t'} - m_{b'} = 55\,\text{GeV}$.

by the symmetry, t_0 and T_0 are no longer mass eigenstates. The mass eigenstates t and T are determined by diagonalization of the mass matrix,

$$(8) \qquad \widehat{M_t} = \begin{pmatrix} \frac{y_t\,v}{\sqrt{2}} & \frac{Y_T\,v}{\sqrt{2}} \\ 0 & M_T \end{pmatrix} = U_L^\dagger \begin{pmatrix} m_t & \\ & m_T \end{pmatrix} U_R,$$

where

$$(9) \qquad \begin{pmatrix} t_X \\ T_X \end{pmatrix} = U_X \begin{pmatrix} t_{0X} \\ T_{0X} \end{pmatrix} = \begin{pmatrix} c_X & -s_X \\ s_X & c_X \end{pmatrix} \begin{pmatrix} t_{0X} \\ T_{0X} \end{pmatrix}, \quad \text{where } X = L, R.$$

The one-loop correction to the hhh coupling constant due to the vectorlike top-quark is evaluated as

$$(10) \qquad \frac{\Gamma_{hhh}^{\text{Vec}}}{\Gamma_{hhh}^{\text{SM}}} \simeq 1 - \frac{N_c m_t^4}{3\pi^2 v^2 m_h^2}\left(\frac{Y_T v}{\sqrt{2}m_T}\right)^2\left[-9 + 6\left(\frac{Y_T v}{\sqrt{2}m_t}\right)^2 + \left(\frac{Y_T v}{\sqrt{2}m_t}\right)^4\right],$$

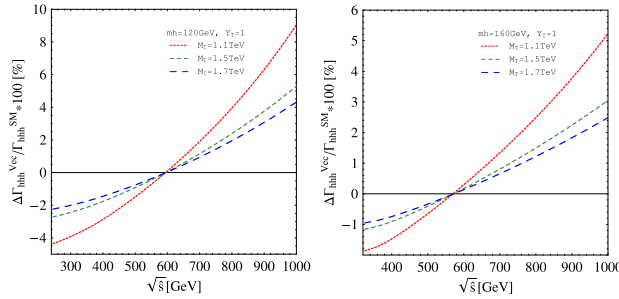Fig. 4. – The rates for one-loop contributions from the vectorlike top-quark T to the hhh coupling constant for $m_h = 120\,\text{GeV}$ (left) and for $m_h = 160\,\text{GeV}$ (right). The t_0–T_0 Yukawa coupling is taken to be $Y_T = 1$, and the gauge invariant mass parameter M_T is chosen as $1100\,\text{GeV}$ (dotted line), $1500\,\text{GeV}$ (dashed line) and $1700\,\text{GeV}$ (long-dashed line), respectively.
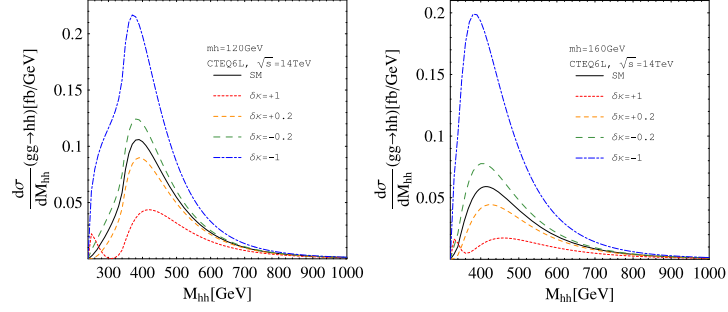
Fig. 5. – The invariant mass distribution of the cross section of $gg \rightarrow hh$ process at the LHC with $\sqrt{s} = 14\,\text{TeV}$ for $m_h = 120\,\text{GeV}$ (left) and $m_h = 160\,\text{GeV}$ (right).

where $y_t^{\text{eff}} = c_L(c_R y_t - s_R Y_T)$. We can see that the correction to the hhh coupling constant decouples as $1/m_T^2$. In fig. 4, the effects on the hhh coupling constant due to the vectorlike top-quark are shown. The stringent experimental bounds from the electroweak precision data impose that mass of T particle is heavy, $m_T \gtrsim 1100\,\text{GeV}$. Therefore, there can be no significant nondecoupling effect on the hhh coupling constant.

3. – Higgs boson pair production

In this section, we discuss Higgs boson pair production processes $gg \rightarrow hh$, $e^+e^- \rightarrow hhZ$, $e^+e^- \rightarrow hh\nu\bar{\nu}$ and $\gamma\gamma \rightarrow hh$ in various new physics models. These processes contain the hhh coupling constant so that they can be used to determine the hhh coupling constant at future collider experiments. The effective hhh coupling constant is parameterized as

$$(11) \qquad\qquad \lambda_{hhh} = \lambda_{hhh}^{\text{SM}}(1 + \Delta\kappa),$$

where $\lambda_{hhh}^{\text{SM}} = -3m_h^2/v$ at the tree level.

At the LHC, the largest cross section of the Higgs boson pair production comes from the gluon fusion mechanism. In fig. 5, we show the invariant mass distributions of the cross section of $gg \rightarrow hh$ process with the deviation of the hhh coupling constant.
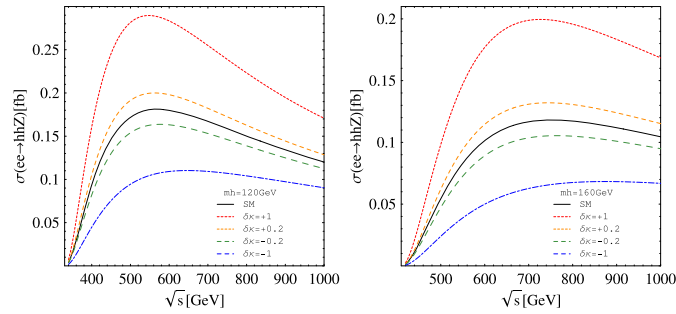

Fig. 6. – The cross sections of $e^+e^- \rightarrow hhZ$ process at the ILC as a function of collision energy $\sqrt{s}$ for $m_h = 120\,\text{GeV}$ (left) and $m_h = 160\,\text{GeV}$ (right).
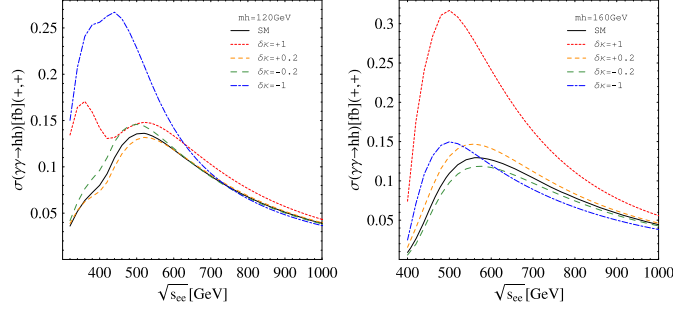
Fig. 7. – The full cross section of $e^-e^-(\gamma(+)\gamma(+)) \to hh$ process as a function of $\sqrt{s}_{ee}$ for $m_h = 120$ GeV (left) and $m_h = 160$ GeV (right).

The total cross section is about 20 (10) fb for $m_h = 120$ (160) GeV in the SM. Only for $\Delta\kappa = +1.0$, a small peak comes from the large hhh coupling constant through the triangular diagram in the near threshold region. The peaks can be found around $M_{hh} \sim 400$ GeV, which are caused by the interference effect of the triangular and the box diagrams. Since these two contributions are destructive to each other, the positive (negative) variation of the hhh coupling constant makes the cross sections small (large) in this process. This means that in the $gg \to hh$ process the sensitivity is getting better for the negative contribution to the hhh coupling constant and vice versa. If we have additional colored particles in the new physics model, this situation could be changed.

At an electron-positron linear collider, the hhh coupling constant will be measured by the double-Higgs-strahlung and the Higgs boson pair production via the W boson fusion mechanism. In fig. 6, the cross sections of the double-Higgs-strahlung are evaluated as a function of e^+e^- center of mass energy $\sqrt{s}$. Under the variation of the hhh coupling constant, the cross section of the double-Higgs-strahlung has the opposite correlation to that of $gg \to hh$. Therefore, the positive contributions to the hhh coupling constant has the advantage to obtain better sensitivities.

At a high energy lepton collider, the hard photons can be obtained from the Compton backscattering method [7]. By using hard photons, Higgs boson pairs can be produced in $\gamma\gamma \to hh$ process. In fig. 7, the full cross sections of $e^-e^-(\gamma(+)\gamma(+)) \to hh$ are shown as a function of the energy of the e^-e^- system. We here choose the same sign polarizations
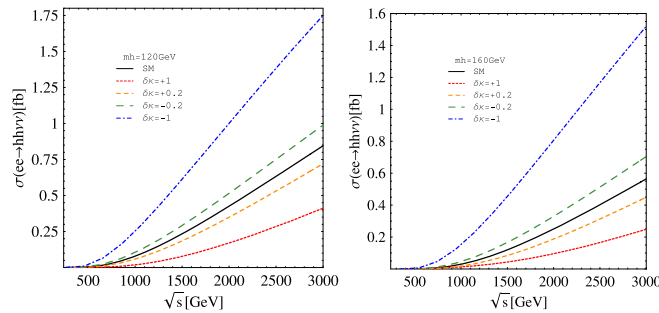

Fig. 8. – The cross sections of $e^+e^- \to hh\nu\bar{\nu}$ process at the ILC as a function of collision energy $\sqrt{s}$ for $m_h = 120$ GeV (left) and $m_h = 160$ GeV (right).

for initial photons in order to efficiently extract information of the hhh coupling constant. The situation is very different from $gg \to hh$ at the LHC. Energies of initial gluons are widely varied at a hadron collider, while backscattered photons at the PLC have narrow band spectra. Therefore, we can tune the effective energy of photons at the PLC to some extent. The relative strength of the W boson and the top-quark loop diagrams strongly depends on the collision energy and the Higgs boson mass. It is found that the negative deviation of the hhh coupling constant makes cross section large for $m_h = 120\,\text{GeV}$ (left), while it has an opposite effect on the cross section for $m_h = 160\,\text{GeV}$ (right).

If we have enough large collision energy at e^+e^- colliders, the Higgs boson pair production via the W boson fusion mechanism becomes important. In fig. 8, we evaluate the production rate for $e^+e^- \to hh\nu\bar{\nu}$ by CalcHEP [8]. For both $m_h = 120\,\text{GeV}$ (left) and $m_h = 160\,\text{GeV}$ (right) cases, the cross section simply scales as a function of energy and can be much larger than those of $e^+e^- \to h\,h\,Z$ and $\gamma\gamma \to h\,h$. The $\Delta\kappa$ dependence in the cross section of $e^+e^- \to hh\nu\bar{\nu}$ is opposite to that in $e^+e^- \to hhZ$; *i.e.* a larger cross section for $e^+e^- \to hh\nu\bar{\nu}$ is obtained for a larger $|\Delta\kappa|$ value with a negative sign.

Model-dependent analyses for the two-Higgs-doublet model, the scalar leptoquark model, the sequential fourth-generation fermion model and the vectorlike quark model can be found in ref. [1].

4. – Conclusion

We have considered the Higgs boson pair production processes, $gg \to hh$, $e^+e^- \to hhZ$, $e^+e^- \to hh\nu\bar{\nu}$ and $\gamma\gamma \to hh$ as a probe of the hhh coupling constant. The measurement of the hhh coupling constant is particularly important to understand the mechanism of the electroweak symmetry breaking. The hhh coupling constant can receive quite large quantum corrections from new physics particles as a nondecoupling effect, which can be an order of more than 100%. Deviations of the hhh coupling constant can give different effects on these processes which can largely modify production cross sections. We have found that these four Higgs boson pair production processes at different colliders can play complementary roles in exploring new physics through the Higgs sector.

REFERENCES

[1] ASAKAWA E., HARADA D., KANEMURA S., OKADA Y. and TSUMURA K., *Phys. Rev. D*, **82** (2010) 115002.
[2] APPELQUIST T. and CARAZZONE J., *Phys. Rev. D*, **11** (1975) 2856.
[3] KENNEDY D. C. and LYNN B. W., *Nucl. Phys. B*, **322** (1989) 1; PESKIN M. E. and TAKEUCHI T., *Phys. Rev. Lett.*, **65** (1990) 964, *Phys. Rev. D*, **46** (1992) 381; ALTARELLI G. and BARBIERI R., *Phys. Lett. B*, **253** (1991) 161.
[4] KANEMURA S., KIYOURA S., OKADA Y., SENAHA E. and YUAN C. P., *Phys. Lett. B*, **558** (2003) 157; KANEMURA S., OKADA Y., SENAHA E. and YUAN C. P., *Phys. Rev. D*, **70** (2004) 115002.
[5] KRIBS G. D., PLEHN T., SPANNOWSKY M. and TAIT T. M. P., *Phys. Rev. D*, **76** (2007) 075016.
[6] GUNION J. F. and HABER H. E., *Phys. Rev. D*, **67** (2003) 075019.
[7] GINZBURG I. F., KOTKIN G. L., PANFIL S. L., SERBO V. G. and TELNOV V. I., *Nucl. Instrum. Methods A*, **219** (1984) 5.
[8] PUKHOV A. *et al.*, arXiv:hep-ph/9908288.